Magnetic microspheres based on glycidyl methacrylate and divinylbenzene modified with different amines for removing chromium VI from aqueous media

Washington José Fernandes Formiga
State University of Rio de Janeiro
Manoel Ribeiro Silva
Federal University of Itajubá
Henrique Almeida Cunha
State University of Rio de Janeiro
Ivana Lourenço Mello Ferreira
State University of Rio de Janeiro
Marcos Antonio Silva Costa
State University of Rio de Janeiro
Jacira Aparecida Castanharo
jaciracastanharo@gmail.com
State University of Rio de Janeiro

Research Article

Keywords: Magnetic microspheres, Glycidyl methacrylate, Divinylbenzene, Amino functionalization, Cr(VI) removal

Posted Date: March 8th, 2024

DOI: https://doi.org/10.21203/rs.3.rs-4003398/v1

Additional Declarations: No competing interests reported.

Abstract

Magnetic microspheres of poly(glycidyl methacrylate-*co*-divinylbenzene) were produced via suspension polymerization. These microspheres were functionalized with ethylenediamine, diethylenetriamine and triethylenetetramine. Microspheres with good morphological control and superparamagnetic behavior were obtained. The Cr (VI) adsorption by the amino functionalized microspheres was pH dependent, achieving better removal results at pH 2. The adsorptive process was best described by the pseudo-second order model. The model confirmed that chemisorption is the main mechanism of adsorption control. The equilibrium isotherm study indicated the best suitability for the Langmuir model. The maximum sorption capacity was 77.35 mg. g^{-1} from the microsphere functionalized with diethylenetriamine, at pH 2, 318.15 K. The adsorbents had ΔH around 40–45 kJ / mol and ΔS between 148–159 J / mol.K. The results indicated an endothermic process, of chemical nature, and with negative ΔG values.

1 Introduction

The treatment of effluents and contaminated liquid media using adsorbent magnetic composites is a simple and low-cost technology. [1–3] Currently, the development of effective chelating copolymers and ion exchangers for selective removal and/or recovery of heavy metal ions from wastewater is of great ecological and economic importance. [4–5] Heavy metals have the ability to accumulate in flora and fauna, causing problems to living beings and the environment.[6] The main activities that generate effluents contaminated with heavy metals are in the industries of metal extraction, metal fabrication, surface finishing, electroplating, paints and pigments, tanneries, fungicides and even the manufacture of batteries. [7–10]

There are several possible treatments for heavy metal. Among the treatments of effluents containing, for example, chromium, reduction and precipitation, ion exchange, adsorption, reverse osmosis and other processes involving membranes can be highlighted. Some of these methods have some disadvantages in terms of high operational cost in addition to the generation of residual sludge. Ranganathan[11] obtained 63% removal of hexavalent chromium from synthetic solutions at pH = 3.0, using coal as an adsorbent. However, its use requires some costly practices for its reuse, such as thermal reactivation at a temperature above 60°C, in addition to presenting contamination by organic products during operation. According to Furtado,[12] the return of the specific use of ion-exchange resins to the detriment of processes with membranes has been due to the characteristic of low salinity Brazilian water, which may not be very favorable to the use of reverse osmosis membranes, which would not justify the use of a technique that accepts input water with high conductivity, and with a lot of organic matter, which increases the chance of membranes biofouling (biological encrustation) with the clogging of the pores decreasing its separating power. Reverse osmosis, with its high sensitivity to organics and chlorine and its strict care, may not be a good alternative in these environments. The removal of ions from water in Brazilian effluents could find in ion exchange a process that requires little equipment, is easy to operate, occupies little space, is highly efficient and can be operated at room temperature, a more viable and economical technique.

Functionalized reticulated magnetic resins consist of a polymer (solid support) with a functional group (binder) such as N, O, S and P, which are atoms capable of coordinating different metal ions (they have active sites with affinity for heavy metals). Therefore, this kind of polymer could remove the pollutants, which will later be agglomerated and attracted by a magnet and removed from the liquid medium, dispensing with the use of filtration or centrifugation normally used in the separation of solids from liquids.[1] The functionalization of these copolymers with amines provides adsorbents with fast kinetics and good selectivity for heavy metal ions, as well as chemical stability and good mechanical strength.[13]

Resins being non-porous and magnetic require smaller diameters to obtain a larger specific area. For this reason, knowledge of the average particle diameter, as well as its control, are necessary in order to design a functionalized copolymer with desired sorption and selectivity performances for heavy metal ions, even later, and may undergo a second chemical modification to obtaining a strong base ion exchange resin. The advantage of amino functionalized cross-linked polymers based on glycidyl methacrylate over conventional ion exchange resins resides in the fact that, depending on the pH, they can adsorb or complex both toxic and precious metals. Thus, in addition to functioning as chelating resins, amino functionalized at acidic pH, these

cross-linked resins can also be used in ion exchange (electrostatic adsorption), because they have primary and secondary amino groups of weak base.[14]

Bruchet *et al*.,[15] sought to find the main experimental factors that affect the conversion yield of the nucleophilic addition of triethylamine into poly(GMA-co-EGDMA). An experimental design was formulated for 5 factors at two levels with eight runs. The factors were: (i) solvent composition (ethanol/DMSO or ethanol/water), (ii) proportion of ethanol in the solvent (v/v), (iii) amine concentration (% v/v), (iv) time reaction time and (v) reaction temperature.

Wieder *et al*.,[16] synthesized chemically modified poly(GMA-co-DVB) monoliths to obtain strong anion exchanger supports. Free epoxide groups were quaternized. When testing the pressure stability of the synthesized monolith, a highly linear dependence between the pressure drop flow rate was obtained, indicating the high stability of the material, even at high flow rates. The strong base anion exchange monoliths produced were highly suitable for the separation of nucleotides and oligonucleotides.

Nastasović *et al*.,[17] synthesized two samples of poly(glycidyl methacrylate-co-ethylene glycol dimethacrylate), poly(GMA-co-EGDMA), with different porosities, by suspension polymerization. Subsequently, they functionalized through a ring-opening reaction of the pendant epoxide groups with ethylenediamine (EDA) and diethylenetriamine (DETA). The sorption kinetics of Cr(VI), Cu(II), Co(II), Cd(II) and Ni(II) were studied under non-competitive conditions (from a single component solutions of the metal salt) and competitive conditions (mixture of different metal solutions). The adsorption of Cr(VI) ions was very fast, presumably because the sorption process occurred predominantly on the surface of amino-functionalized granules, with no diffusion of oxyanions into the resin pores, a fact confirmed by the poor fit of the intraparticle diffusion model .

Although there are works in the literature describing the synthesis of magnetic polymeric microspheres based on functionalized glycidyl methacrylate (GMA) and divinylbenzene (DVB),[18–22] no work has been found on the influence of the chain size of the amine groups in amino functionalized magnetic copolymers based in GMA and DVB for chromium (VI) removal from aqueous medium.

2 Results and Discussion

2.1 Characterization of the material

The elemental analysis (EA) results for magnetic poly (glycidyl methacrylate-*co*-divinylbenzene) (P(GMA-*co*-DVB)-M) before modification (R14) and the samples modified with ethylenediamine (R14-EDA), diethylenetriamine (R14-DETA) and triethylenetetramine (R14-TETA) are presented in Table 1. In the R-14 copolymer, a substantial amount of epoxy groups could be obtained, which would consequently lead to more amino groups attached to the surface of the copolymers, The increase in the nitrogen content in all the amino-functionalized copolymers corroborated for the chemical modification success, demonstrating that amino groups introduction in the magnetic poly(GMA-*co*-DVB) microspheres occurred. It can also be noted that the functionalized amino resin with triethylenetetramine (R14-TETA) showed the highest nitrogen content, since this amine has four amino groups, but with less use in the opening of the epoxide rings, thus obtaining the lowest yield.

Table 1
Elemental analysis of the P(GMA-*co*-DVB)-M before (R14) and after functionalization with ethylenediamine (R14-EDA), diethylenetriamine (R14-DETA) and triethylenetetramine (R14-TETA).

Copolymer	% C	% H	% N	% Others
R14[a)]	54.50	11.10	0.10	34.30
R14-EDA	50.70	9.80	6.50	33.00
R14-DETA	50.51	11.22	6.98	31.29
R14-TETA	50.33	9.52	7.71	32.44

[a)]R14: GMA/DVB = 98/2; BPO = 1%; [iron oxide] = 10%; T = 80°C.

Figure 1 shows the FTIR-ATR spectra obtained for all samples. Characteristic bands can be observed between 1720–1729 cm^{-1} (υC = O), which corresponds to the GMA ester carbonyl absorption band. The bands at 847 and 992 cm^{-1} are attributed to epoxide groups in copolymer R14. After the ring-opening reaction with the different amines, new bands appeared at 1560, 1559 and 1555 cm^{-1}, which correspond to the δN-H vibrations in the copolymers R14-EDA, R14-DETA and R14-TETA, respectively. These results clearly indicated that the ester groups successfully reacted with the amines. A band referring to the secondary amine appeared around 3225–3295 cm^{-1} for all amino functionalized copolymers. Although the υNH_2 vibrations could appear as a sharp band and weak intensity, bands of υOH are broad and of strong intensity in the region between 3500-3400cm^{-1}. Thus, the vibrations for these groups may have overlapped.[13] The absorption bands found at approximately 847 and 992 cm^{-1} (epoxide ring vibrations), 1255–1259 and 1455 cm^{-1} (δ(CH) of the epoxide group), for the three functionalized copolymers, did not completely disappear from the samples spectra. They can be attributed to the epoxide groups located inside the microspheres that were inaccessible to react with the amines. [13]

Figure 2 shows P(GMA-*co*-DVB)-M scanning electron microscopy (SEM) images for all samples. As can be seen, there were no significant changes in the morphology material. Its spherical shape remained, indicating good structural resistance during chemical modification methodology. Apparently, the magnetic particles were distributed over the microspheres surface, grouped in small dots, instead of randomly distributed. Similar results were found in the literature.[23–25]

Table 2 presents the diameter, magnetic properties and thermal resistance of microspheres results obtained. As can be seen, there wasn't significant change in the microspheres average size (d(0.5)). This result indicates that no fragmentation or agglomeration occurred during the chemical modification reactions. In the magnetization results presented, copolymer R14 was found to have twice the saturation magnetization (M_S) compared to the modified copolymers. As M_S is directly proportional to the amount of magnetic material incorporated, it is possible that the lower values found for the chemically modified microspheres were caused by the leaching of the iron oxide located on their surface, during the chemical reactions.[26] Similar M_S values were also found for chemically modified copolymers based on styrene and divinylbenzene by other authors.[27] The M_R/M_S (residual magnetization/ saturation magnetization) ratio is also presented in Table 2. All values are considered low and indicate an appreciable amount of superparamagnetic particles contained in the microspheres.[28] This characteristic is very important because it guarantees that the microspheres will not remain agglomerated after the magnetic field were removed after the separation process. If they remained clustered, it would make their regeneration difficult. Table 2 also presented the P-(GMA-*co*-DVB)-M thermogravimetric analysis (TGA) results for all samples. Apparently, the amino groups incorporation did not cause any change in the initial degradation temperature (T_{onset}) and also the temperature of maximum degradation rate (T_{max}) since the equipment error is ± 4%. The mass loss can be attributed to degradation of the organic material in the copolymer. These residues showed great similarity to the point of being considered equal when taking into account the random error of the equipment, with the exception of the copolymer functionalized with triethylenetetramine, in which the difference in relation to the R14 copolymer was about 31% increment. The material obtained as waste probably is iron, which was added in the form of an oxide to give the final material the required magnetic property. The in situ copolymerization was prepared with particulate iron oxides and their distribution in the resin is completely random, thus it is to be expected that the level of incorporation of the magnetic material does not have a biased behavior, and varying iron contents can even be obtained for the same series of measures.

Table 2
P(GMA-co-DVB)-M average size, magnetic properties, and thermal degradation results before (R14) and after functionalization with ethylenediamine (R14-EDA), diethylenetriamine (R14-DETA) and triethylenetetramine (R14-TETA)

Microspheres	d(0.5)[a] [µm]	M_S[b] [emu/g]	M_R[c] [emu/g]	M_R/ M_S	T_{onset} [°C]	T_{max} [°C]	Residual [% mass]
R14	101.62	4.76	0.43	0.090	293	315	11.59
R14-EDA	100.61	2.25	0.25	0.111	294	317	11.69
R14-DETA	99.78	2.20	0.24	0.109	302	323	10.33
R14-TETA	97.30	2.20	0.25	0.114	306	325	15.21

[a]d(0.5) - average basic diameter; [b]M_S - saturation magnetization; [c]M_R - residual magnetization;.

2.2 Effect of pH on the adsorption of Cr (VI) in the amino magnetic copolymers

The pH effect on the chromium (VI) adsorption by the amino functionalized copolymers R14-EDA, R14-DETA and R14-TETA is shown in Fig. 3. It can be seen from the graph that the optimum range of adsorption of Cr (VI) ions by the three different adsorbents occurred in the acidic pH range, that is, at pH below 6. Its optimized range was in pH = 2. Already witch the pH increase (above 6), the adsorption of Cr (VI) ion showed, for all amino functionalized copolymers, a decrease in adsorption until reaching strongly alkaline pHs. The pH is an important factor affecting the adsorption behavior of adsorbents because of its effect on the surface charge of the adsorbents and the conversion of the metal ion species.[29] Bayramoglu *et al.*[30] showed that the adsorption of chromium (VI) ions depends on the protonation or deprotonation of amino groups on the microspheres surface. In aqueous solutions, Cr (VI) exists in the form of chromic acid (H_2CrO_4) and in the form of dichromate ($Cr_2O_7^{2-}$) in the following equilibrium:

$H_2CrO_4 \leftrightarrow HCrO_4^- + H^+$, $k_1 = 1.21$ (1)

$Cr_2O_7^{2-} + H_2O \leftrightarrow 2\ HCrO_4^-$, $k_2 = 35.5$ (2)

There may also be several anionic forms, such as:

$HCrO_4^- \leftrightarrow CrO_4^{2-} + H^+$, $k_3 = 3 \times 10^{-7}$ (3)

$HCrO_7^- \leftrightarrow CrO_7^- + H^+$, $k_4 = 0.85$ (4)

Chromium hexavalent (Cr(VI)), behaves as an oxyanion according to its aqueous chemistry and these species fraction is dependent on chromium concentration and pH's solution.[31] Anionic forms, such as chromate (CrO_4^{2-}) can be adsorbed on pH > 6, dichromate ($Cr_2O_7^{2-}$) and hydrogenchromate ($HCrO_4^-$) on pH between 1–6.[32][20] Therefore, the distribution species of Cr (VI) could be the main variable for Cr (VI) ions removal by adsorbent. The functional amino groups on the magnetic microspheres surface could determine the type of electrostatic interaction between the metal ion and the sorbent surface for Cr (VI) adsorption. In addition,, at lower pH values, the protonated amine group of amino magnetic microphores which leads to an increased electrostatic attraction between NH_3^+ and the sorbate anion.[31] Thus, at acidic pH, the amino groups of the adsorbent microspheres, R14-EDA, R14-DETA and R14-TETA can be positively charged, which leads to an electrostatic attraction with the negatively charged chromium (VI) species, since the main species at lower pH is $HCrO_4^-$. It is concluded that pH dependency for Cr (VI) was a protic equilibrium in which the protonated $HCrO_4^-$ species of the oxyanions influenced the adsorption.

Figure 3 also presented the pH dependence on the Cr (VI) removal rate. Under the studied conditions, it was observed that at pH = 2 showed the best results of Cr (VI) removal efficiency. According to Malovic *et al.*,[13] under the same reaction conditions, the

degree of conversion of epoxide groups decreases in order from ethylenediamine to triethylenetetramine. This could be expected, since the limitation of the reaction occurs due to a steric impediment effect, which is one of the main problems in the functionalization of adsorbents with larger groups. However, this phenomenon was not observed in this work. R14-DETA had the highest efficiency in metal removal with 98.4% removal (pH = 2), compared to R14-EDA wich 89.6% maximum removal rate at same pH. The best result may be due to the presence of protonated amino groups substantial amount on these copolymer surface.

2.3 Adsorption isotherms of the amino magnetic copolymers

The experimental adsorption isotherms for different temperatures (298.15, 303.15, 308.15, 313.15 and 318.15 K) are shown in Fig. 4 and the results of the adjustments made for both models, Langmuir and Freundlich, are presented in the Table 3. As can be seen, the experimental data fit better to Langmuir than Freundlich model. This is because it presented correlation coefficients closer to one. The parameters q_{max} ($mg.g^{-1}$) and K_L ($L.mg^{-1}$) are the Langmuir constants associated, respectively, with the capacity and the adsorption energy. It is also known that the temperature increase is inversely proportional to the reaction medium viscosity. As a consequence, there is an increase in the kinetic energy and diffusion of the solute molecules into the adsorbent in adsorption phenomena, thus favoring the mass transfer from molecules over external layer and inside the adsorbent particles internal pores.[33]

To calculate the maximum adsorbed capacity (q_{max}) and the adsorption constant (K_L), the Langmuir model was adopted. [34–35] Comparing the three copolymers in the same temperature range, the R14-DETA showed the best results in the Cr (VI) adsorption and also the lowest values of the K_L parameter, at the same temperature, indicating that it is the copolymer which requires the least energy to carry out the adsorption. The maximum adsorption value estimated was 78.21 $mg.g^{-1}$, at 45°C (318.15 K). As can be seen, in Fig. 4, in general, the temperature increase favored the Cr (VI) adsorption in all amino functionalized copolymers, regardless the original amino group size and/ou the amino groups number bonded to the copolymer (EDA – two amino groups; DETA – three amino groups; TETA – four amino groups). Comparing the three copolymers at the same temperature range, the R14-DETA copolymer also presented the best results in Cr(VI) adsorption. Huang *et al.*[36] reported a DETA functionalized magnetic adsorbent which was prepared by the covalent binding of polyacrylic acid (PAA) and obtained maximum Cr(VI) adsorption capacity (q_{max}) from 11.24$mg.g^{-1}$ at 25º C. Another similar EDA functionalized adsorbent, based on magnetic glycidyl methacrylate, presented q_{max} = 61.35 $mg.g^{-1}$ at 35 º C.[21] Comparing these literature results with those obtained in this work, at the same temperatures, it can be observed that both EDA copolymer (R14-EDA) and DETA copolymer (R-14-DETA) presented more significant adsorption values (60.35 $mg.g^{-1}$ at 25 º C and 73.20 $mg.g^{-1}$ at 35 º C, respectively).The results presented in this stage are consistent with the elementar analysis results as described in Table 1 for all amino functionalized copolymers. It is possible to notice that when the nitrogen percentage increase in R14-EDA (N = 6.50%) and R14-DETA (N = 6.98%) their q_{max} values also increases in all temperatures, at the same order. Although R14-TETA showed greater nitrogen incorporation (N = 7.71%), such an event was not observed in its q_{max} values. This can be explained by the steric impediment effect caused by the presence of larger groups in this copolymer.[13] Possibly not all amino groups present in R14-TETA were available in Cr (VI) adsorption process. These results showed that the amino groups played a very important role in the Cr (VI) adsorption process. The q_{max} increase values can also indicated a prominence of amino groups available in the copolymers synthesized in this work, which are promising particles for the Cr (VI) removal in wastewater.

Table 3
Parameters of adjustments to the Langmuir and Freundlich models for different temperatures used in the Cr (VI) adsorption by P(GMA-co-DVB)-M: functionalization with ethylenediamine (R14-EDA), diethylenetriamine (R14-DETA) and triethylenetetramine (R14-TETA).

		Copolymer		q_{max} [a] [mg/g]	K_L [b] [L/mg]	R^2 [c]		K_F [d] [(mg/g)(L/mg)$^{1/n}$]	N [e]	R^2
Temperature [K]	298.15	R14-EDA	Langmuir	60.97	0.060	0.999	Freundlich	0.667	2.642	0.940
		R14-DETA		64.23	0.054	0.996		1.209	2.796	0.909
		R14-TETA		56.33	0.061	0.989		1.342	2.662	0.785
	303.15	R14-EDA		69.77	0.085	0.992		1.963	2.873	0.877
		R14-DETA		71.87	0.076	0.994		1.679	2.893	0.833
		R14-TETA		57.70	0.086	0.993		1.978	2.623	0.903
	308.15	R14-EDA		72.08	0.101	0.997		2.283	2.677	0.898
		R14-DETA		74.12	0.096	0.994		2.168	2.636	0.921
		R14-TETA		57.87	0.103	0.988		2.420	2.444	0.799
	313.15	R14-EDA		74.40	0.125	0.996		2.875	2.281	0.919
		R14-DETA		77.02	0.120	0.995		2.752	2.633	0.862
		R14-TETA		58.62	0.128	0.993		2.904	2.665	0.832
	318.15	R14-EDA		76.03	0.185	0.995		4.222	2.165	0.923
		R14-DETA		78.21	0.178	0.978		4.098	1.993	0.896
		R14-TETA		58.65	0.188	0.975		4.331	1.981	0.789

[a] q_{max}: solid phase maximum solute adsorption capacity ($mg.g^{-1}$); [b] K_L: separation factor; [c] R^2: correlation coefficient; [d] K_F: Freundlich constant pre-exponential; [e] N: Freundlich isotherm exponent.

2.4 Adsorption kinetics of Cr (VI) in the amino magnetic copolymers

In order to investigate the controlling mechanism of Cr(VI) adsorption process, kinetic models were used and validated by the correlation coefficients of their linearized equations: [log (qe - qt) vs t] for the pseudo-first order model, [t/qt vs t] for the pseudo-second order model and [qt vs $t^{1/2}$] for the intraparticle diffusion model. All the kinetic parameters obtained for each model, where K_{o1} (min^{-1}) represents the adsorption kinetic rate constant for the pseudo-first order model, K_{o2} ($g\ mg^{-1}.\ min^{-1}$) is the adsorption kinetic rate constant for the pseudo-second order model and K_d is the rate constant in the intraparticle diffusion model. The correlation coefficients and linearized equations of these three kinetic models for the R14 copolymer functionalized by the three different amines (R14-EDA, R14-DETA and R14-TETA) are presented in Tables 4–6. As can be seen that in all the three kinetic models fitted, the reaction rates increased with increasing temperature for all the functionalized copolymers studied. It was also observed at the temperatures analyzed, the experimental data had the best fits provided by the pseudo-second order model, with the R^2 correlation coefficients obtained closer to one (R^2=0.99) for most of copolymers. In this model, the Cr (VI) concentration adsorbed at equilibrium is a function of the initial metal ions concentration and the interaction nature between the adsorbent and the adsorbate. Then the adsorption process is controlled by the surface reaction with the speed mechanism being chemisorption involving valence forces through the sharing or electrons between the amino functionalized copolymers and Cr (VI).[37]

Figure 5 shows the variation of Cr(VI) concentrations in the liquid phase (C/C_o) as a function of the contact time of the different amino magnetic copolymers. C and C_o correspond to the concentration of the metals at time t and at the initial concentration. In

line to Sun and Xu,[38] the first stage of adsorption can be affected by the adsorbate concentration and agitation. Therefore, increasing the concentration of the adsorbate in the initial part can accelerate its diffusion from the solution to the surface of the adsorbent. Next, adsorption becomes dependent on the nature of the adsorbate molecules. At the end of the process, the third stage is generally considered the determining stage, depending on the nature of the adsorbent, as its reactive sites can been saturated. It was possible to observe that the adsorption of Cr (VI) followed this pattern described in the literature. It was faster in the initial stage and becomes slower when approaching the final equilibrium. It is also possible to observe that equilibrium for Cr(VI) removal occurred in approximately 300 min for all amino-functionalized copolymers. The equilibrium point occurs because over time, the number of empty sites decreases, which reduces the percentage of Cr (VI) removal until its equilibrium. Otherwise, the adsorbent sites became saturated and, from that moment on, the sorption became slow in later time intervals.[7] The adsorption speed was directly proportional to the concentration gradient, as the saturation of the adsorption sites occurs, the concentration decrease.[39–40] The control of the adsorption mechanism of this process is chemisorption, involving valence forces through the sharing or exchange of electrons between the adsorbent and the adsorbate. [41]

Table 4
R14-EDA copolymer velocity constants obtained in the kinetic fits for temperatures of 298, 303, 308, 313 and 318K.

T = 298.15 [K]				
	C_0 = 50 mg/L	C_0 = 100 mg/L	C_0 = 200 mg/L	$\bar{x}$
Pseudo-first order	K_{o1}=0.0053	K_{o1}= 0.0053	K_{o1}=0.0054	$\bar{x}$
	R^2 = 0.831	R^2 = 0.729	R^2 = 0.792	$K_{o1} = 0.0053$
Pseudo-second Order	K_{o2}=0.000121	K_{o2}=0.000120	K_{o2}=0.000121	$\bar{x}$
	R^2 = 0.999	R^2 = 0.999	R^2 = 0.999	$K_{o2} = 0.000121$
Intraparticle diffusion	K_d=3.591	K_d=3.222	K_d=3.526	$\bar{x}$
	R^2 = 0.699	R^2 = 0,771	R^2 = 0.622	$K_d = 3.446$
T = 303.15 [K]				
	C_0 = 50 mg/L	C_0 = 100 mg/L	C_0 = 200 mg/L	$\bar{x}$
Pseudo-first order	K_{o1}=0.0054	K_{o1}=0.0055	K_{o1}=0.0058	$\bar{x}$
	R^2 = 0.782	R^2 = 0.726	R^2 = 0.819	$K_{o1} = 0.0057$
Pseudo-second Order	K_{o2}=0.000150	K_{o2}=0.000153	K_{o2}=0.000149	$\bar{x}$
	R^2 = 0.999	R^2 = 0.995	R^2 = 0.991	$K_{o2} = 0.000151$
Intraparticle diffusion	K_d=3.622	K_d=3.321	K_d=3.499	$\bar{x}$
	R^2 = 0.698	R^2 = 0.592	R^2 = 0.751	$K_d = 3.481$
T = 308.15 [K]				
	C_0 = 50 mg/L	C_0 = 100 mg/L	C_0 = 200 mg/L	$\bar{x}$
Pseudo-first order	K_{o1}=0.0062	K_{o1}=0.0059	K_{o1}=0.0064	$\bar{x}$
	R^2 = 0.783	R^2 = 0.834	R^2 = 0.813	$K_{o1} = 0.0062$
Pseudo-second Order	K_{o2}=0.000168	K_{o2}=0.00171	K_{o2}=0.00165	$\bar{x}$
	R^2 = 0.999	R^2 = 0.999	R^2 = 0.996	$K_{o2} = 0.000168$
Intraparticle diffusion	K_d=3.821	K_d=3.802	K_d=3.912	$\bar{x}$
	R^2 = 0.785	R^2 = 0.692	R^2 = 0.721	$K_d = 3.845$
T = 313.15 [K]				

T = 298.15 [K]				
	C_0 = 50 mg/L	C_0 = 100 mg/L	C_0 = 200 mg/L	$\bar{x}$
Pseudo-first order	K_{o1}=0.0066 R^2 = 0.852	K_{o1}=0.0062 R^2 = 0.846	K_{o1}=0.0068 R^2 = 0.899	$\bar{K}_{o1} = 0.0065$
Pseudo-second Order	K_{o2}=0.000198 R^2 = 0.999	K_{o2}=0.000197 R^2 = 0.991	K_{o2}=0.000200 R^2 = 0.994	$\bar{K}_{o2} = 0.000198$
Intraparticle diffusion	K_d=4.022 R^2 = 0.721	K_d=3.991 R^2 = 0,763	K_d=3.906 R^2 = 0.761	$\bar{K}_d$= 3.973
T = 318.15 [K]				
	C_0 = 50 mg/L	C_0 = 100 mg/L	C_0 = 200 mg/L	$\bar{x}$
Pseudo-first order	K_{o1}=0.0070 R^2 = 0.859	K_{o1}=0.0071 R^2 = 0.879	K_{o1}=0.0071 R^2 = 0.739	$\bar{K}_{o1} = 0.0071$
Pseudo-second Order	K_{o2}=0.000212 R^2 = 0.990	K_{o2}=0.000215 R^2 = 0.999	K_{o2}=0.000210 R^2 = 0.991	$\bar{K}_{o2} = 0.000207$
Intraparticle diffusion	K_d=3.991 R^2 = 0.690	K_d=4.130 R^2 = 0,732	K_d=4.119 R^2 = 0.729	$\bar{K}_d = 4.080$

R14: GMA/DVB = 98/2; BPO = 1%; iron oxide = 10%; T = 80°C; EDA - ethylene diamine, 24h, pH = 2.

Table 5
R14-DETA copolymer velocity constants obtained in the kinetic fits for temperatures of 298, 303, 308, 313 and 318K.

T = 298.15 [K]				
	C_0 = 50 mg/L	C_0 = 100 mg/L	C_0 = 200 mg/L [1]	$\bar{x}$
Pseudo-first order	K_{o1}=0.0059	K_{o1}= 0.0055	K_{o1}=0.0053	$\bar{x}$
	R^2 = 0.921	R^2 = 0.834	R^2 = 0.899	$K_{o1} = 0.0056$
Pseudo-second Order	K_{o2}=0.000131	K_{o2}=0.000130	K_{o2}=0.000129	$\bar{x}$
	R^2 = 0.999	R^2 = 0.993	R^2 = 0.997	$K_{o2} = 0.000129$
Intraparticle diffusion	K_d=3.896	K_d=3.937	K_d=3.752	$\bar{x}$
	R^2 = 0.956	R^2 = 0.977	R^2 = 0.893	$K_d = 3.862$
T = 303.15 [K]				
	C_0 = 50 mg/L	C_0 = 100 mg/L	C_0 = 200 mg/L	$\bar{x}$
Pseudo-first order	K_{o1}=0.0061	K_{o1}=0.0059	K_{o1}=0.0061	$\bar{x}$
	R^2 = 0.930	R^2 = 0,926	R^2 = 0.935	$K_{o1} = 0.0060$
Pseudo-second order	K_{o2}=0.000165	K_{o2}=0.000163	K_{o2}=0.000167	$\bar{x}$
	R^2 = 0.997	R^2 = 0.994	R^2 = 0.999	$K_{o2} = 0.000165$
Intraparticle diffusion	K_d=3.899	K_d=4.031	K_d=4.036	$\bar{x}$
	R^2 = 0.932	R^2 = 0.918	R^2 = 0.893	$K_d = 3.989$
T = 308.15 [K]				
	C_0 = 50 mg/L	C_0 = 100 mg/L	C_0 = 200 mg/L	$\bar{x}$
Pseudo-first order	K_{o1}=0.0068	K_{o1}=0.0069	K_{o1}=0.0065	$\bar{x}$
	R^2 = 0.912	R^2 = 0.931	R^2 = 0.917	$K_{o1} = 0.0067$
Pseudo-second order	K_{o2}=0.000188	K_{o2}=0.00189	K_{o2}=0.00189	$\bar{x}$
	R^2 = 0.999	R^2 = 0.989	R^2 = 0.993	$K_{o2} = 0.000189$
Intraparticle diffusion	K_d=3.913	K_d=3.935	K_d=4.168	$\bar{x}$
	R^2 = 0.894	R^2 = 0.898	R^2 = 0.831	$K_d = 4.005$
T = 313.15 [K]				

T = 298.15 [K]				
	C_0 = 50 mg/L	C_0 = 100 mg/L	C_0 = 200 mg/L	$\bar{x}$
Pseudo-first order	K_{o1}=0.0073 R^2 = 0.962	K_{o1}=0.0073 R^2 = 0.954	K_{o1}=0.0077 R^2 = 0.946	$\bar{K}_{o1} = 0.0074$
Pseudo-second order	K_{o2}=0.000221 R^2 = 0.995	K_{o2}=0.000220 R^2 = 0.999	K_{o2}=0.000223 R^2 = 0.997	$\bar{K}_{o2} = 0.000221$
Intraparticle diffusion	K_d=4.120 R^2 = 0.912	K_d=4.032 R^2 = 0.923	K_d=4.199 R^2 = 0.916	$\bar{K}_d$= 4.117
T = 318.15 [K]				
	C_0 = 50 mg/L	C_0 = 100 mg/L	C_0 = 200 mg/L	$\bar{x}$
Pseudo-first order	K_{o1}=0.0077 R^2 = 0.953	K_{o1}=0.0079 R^2 = 0.962	K_{o1}=0.0081 R^2 = 0.932	$\bar{K}_{o1} = 0.0079$
Pseudo-second order	K_{o2}=0.000239 R^2 = 0.999	K_{o2}=0.000243 R^2 = 0.998	K_{o2}=0.000237 R^2 = 0.999	$\bar{K}_{o2} = 0.000240$
Intraparticle diffusion	K_d=4.211 R^2 = 0.702	K_d=4.236 R^2 = 0.713	K_d=4.310 R^2 = 0.721	$\bar{K}_d = 4.252$

R14: GMA/DVB = 98/2; BPO = 1%; iron oxide = 10%; T = 80°C; DETA - diethylene triamine, 24h, pH = 2.

Table 6
R14-TETA copolymer velocity constants obtained in the kinetic fits for temperatures of 298, 303, 308, 313 and 318 K.

T = 298.15 [K]				
	C_0 = 50 mg/L	C_0 = 100 mg/L	C_0 = 200 mg/L	$\bar{x}$
Pseudo-first order	K_{o1}=0.0050 R^2 = 0.759	K_{o1}= 0.0051 R^2 = 0.751	K_{o1}=0.0052 R^2 = 0.741	$\bar{x}$ $\mathrm{K_{o1}} = 0.0051$
Pseudo-second order	K_{o2}=0.000117 R^2 = 0.999	K_{o2}=0.000116 R^2 = 0.999	K_{o2}=0.000115 R^2 = 0.999	$\bar{x}$ $\mathrm{K_{o2}} = 0.000117$
Intraparticle diffusion	K_d=3.389 R^2 = 0.694	K_d=3.369 R^2 = 0.592	K_d=3.367 R^2 = 0.623	$\bar{x}$ $\mathrm{K_d} = 3.375$
T = 303.15 [K]				
	C_0 = 50 mg/L	C_0 = 100 mg/L	C_0 = 200 mg/L	$\bar{x}$
Pseudo-first order	K_{o1}=0.0053 R^2 = 0.856	K_{o1}=0.0053 R^2 = 0.890	K_{o1}=0.0052 R^2 = 0.793	$\bar{x}$ $\mathrm{K_{o1}} = 0.0053$
Pseudo-second order	K_{o2}=0.000143 R^2 = 0.999	K_{o2}=0.000143 R^2 = 0.990	K_{o2}=0.000141 R^2 = 0.999	$\bar{x}$ $\mathrm{K_{o2}} = 0.000143$
Intraparticle diffusion	K_d=3.471 R^2 = 0.629	K_d=3.396 R^2 = 0.758	K_d=3.421 R^2 = 0.681	$\bar{x}$ $\mathrm{K_d} = 3.429$
T = 308.15 [K]				
	C_0 = 50 mg/L	C_0 = 100 mg/L	C_0 = 200 mg/L	$\bar{x}$
Pseudo-first order	K_{o1}=0.0059 R^2 = 0.709	K_{o1}=0.0055 R^2 = 0.793	K_{o1}=0.0049 R^2 = 0.831	$\bar{x}$ $\mathrm{K_{o1}} = 0.0054$
Pseudo-second order	K_{o2}=0.000161 R^2 = 0.999	K_{o2}=0.00159 R^2 = 0.993	K_{o2}=0.00163 R^2 = 0.988	$\bar{x}$ $\mathrm{K_{o2}} = 0.000161$
Intraparticle diffusion	K_d=3.511 R^2 = 0.793	K_d=3.536 R^2 = 0.863	K_d=3.613 R^2 = 0.861	$\bar{x}$ $\mathrm{K_d} = 3.553$
T = 313.15 [K]				

T = 298.15 [K]				
	C_0 = 50 mg/L	C_0 = 100 mg/L	C_0 = 200 mg/L	$\bar{x}$
Pseudo-first order	K_{o1}=0.0073	K_{o1}=0.0073	K_{o1}=0.0077	$\bar{K}_{o1} = 0.0074$
	R^2 = 0.795	R^2 = 0.798	R^2 = 0.827	
Pseudo-second order	K_{o2}=0.000188	K_{o2}=0.000188	K_{o2}=0.000192	$\bar{K}_{o2} = 0.000189$
	R^2 = 0.999	R^2 = 0.998	R^2 = 0.999	
Intraparticle diffusion	K_d=3.549	K_d=3.594	K_d=3.548	$\bar{K}_d$= 3.564
	R^2 = 0.862	R^2 = 0.887	R^2 = 0.894	
T = 318.15 [K]				
	C_0 = 50 mg/L	C_0 = 100 mg/L	C_0 = 200 mg/L	$\bar{x}$
Pseudo-first order	K_{o1}=0.0067	K_{o1}=0.0069	K_{o1}=0.0068	$\bar{K}_{o1} = 0.0068$
	R^2 = 0.795	R^2 = 0.713	R^2 = 0.709	
Pseudo-second order	K_{o2}=0.000202	K_{o2}=0.000203	K_{o2}=0.000201	$\bar{K}_{o2} = 0.000202$
	R^2 = 0.999	R^2 = 0.999	R^2 = 0.999	
Intraparticle diffusion	K_d=3.663	K_d=3.599	K_d=3.702	$\bar{K}_d = 3.654$
	R^2 = 0.895	R^2 = 0.910	R^2 = 0.879	

R14: GMA/DVB = 98/2; BPO = 1%; iron oxide = 10%; T = 80°C; TETA - triethylene tetramine, 24h, pH = 2.

2.5 Thermodynamic parameters determination of Cr (VI) in the amino magnetic copolymers

The thermodynamic parameters of adsorption have been studied at a range of 298.15 to 318.15 K. The results obtained were presented in the in Table 7. As can be observed, the increase in temperature favored the removal of Cr (VI) oxyanions from the solution, considering that the free energy values increased in modulus. Ghasemlou *et al.*[42] explained that the increase in collisions leading to a greater adsorption capacity. Among the three copolymers evaluated, the adsorbent R14-EDA was the most favored with the increase in temperature from 25 to 45°C, there was an increase in free energy of 123%. The negative ΔG° values presented confirm its spontaneous nature and the adsorption process feasible, since the increase in ΔG° modulus is directly proportional to temperature. The results demonstrated that the processes are designed to form electrostatic interactions and/or chromium-adsorbent complexes.[31] This results indicated a Cr (VI) high affinity for the adsorbent copolymer.[43] The standard enthalpy values (ΔH◦) for the adsorption of Cr(VI) were 41.51 kJ/mol (R14-EDA), 44.80 kJ/mol (R14-DETA) and 41.85 kJ/mol (R14-TETA), while the standard entropy (ΔS◦) were 148.32 J/mol.K, 159.42 J/mol.K and 150.55 J/mol.K, respectively. The ΔH◦ positive value showed that Cr(VI) adsorption is an endothermic process. Already, the ΔS◦ positive results indicated that randomness increases at the solid/solution interface during the Cr(VI) adsorption on magnetic amino copolymers. The R14-DETA adsorbent presented the highest ΔH° value, which indicates that it has a higher binding energy with the Cr (VI). The positive values of ΔH° and ΔS° suggest that entropy contributed more than enthalpy to obtain negative values of ΔG°. The magnitude of ΔH° can also confirm the nature of the adsorption, that is, above 20.9 kJ.mol^{-1} suggests that the adsorption process is chemical

and corroborated to kinetic models.[44] Through these results, it is possible to conclude that all amino magnetic copolymers synthesized in this work can be used as adsorbent in conventional processes for water or effluents decontamination containing hexavalent chromium (Cr (VI)).

Table 7
Equilibrium parameters for calculating the Gibbs free energy of the assortative process and analysis of the thermodynamic parameters of the Gibbs equation in the Cr (VI) adsorption by P(GMA-*co*-DVB)-M: functionalization with ethylenediamine (R14-EDA), diethylenetriamine (R14-DETA) and triethylenetetramine (R14-TETA).

Temperature [K]	ln[55,5*K_L]	ΔG° [KJ.mol^{-1}]	ΔH° [KJ.mol^{-1}]	ΔS° [J.mol^{-1}.K^{-1}]	R^2		
Copolymers	R14-EDA	298.15	1.205	-2986.08			
		303.15	1.551	-3909.83			
		308.15	1.724	-4416.17	41,510.14	148.32	0.979
		313.15	1.937	-5042.88			
		318.15	2.329	-6160.39			
	R14-DETA	298.15	1.098	-2720.78			
		303.15	1.439	-3627.75			
		308.15	1.673	-4286.10	44,799.16	159.42	0.988
		313.15	1.896	-4936.60			
		318.15	2.290	-6058.36			
	R14-TETA	298.15	1.216	-3014.78			
		303.15	1.563	-3939.31			
		308.15	1.743	-4466.41	41,846.86	150.55	0.982
		313.15	1.961	-5104.63			
		318.15	2.345	-6202.94			

3 Conclusion

This work presented an understanding of Cr (VI) adsorptive process, as well as the different magnetic adsorbents synthesis, with a weak base (amino functionalized). During the copolymers amino functionalization, their magnetic properties was maintaining, as well their superparamagnetism and thermal resistance. The results demonstrated that the Cr (VI) adsorption process depends on the pH in amino functionalized adsorbents. It was also possible, identifying the phenomenon nature involved in the process, to predict adsorbed chromium species. All amino magnetic copolymers have great potential to be used as Cr (VI) adsorbents in aqueous media. However, the R14-DETA presented the most maximum removal capacity (q_{max}) of 63.95 mg.g^{-1} at 298.15 K and 77.35 mg. g^{-1} at 318.15 K. The kinetic modeling showed as the Cr (VI) adsorption process from aqueous solutions effectiveness strongly depends on the adsorption dynamics. Thermodynamic studies showed that the Cr (VI) adsorption in the functionalized copolymers presented 41.5 kJ/mol < ΔH > 44.8 kJ/mol and 148 J/mol.K < ΔS > 159 J/mol.K. The results indicated an endothermic process, of a chemical nature, with energetically favorable sorption, with negative ΔG values with growth in module with increasing temperature. The adsorptive process became more favorable with increasing temperature and despite being endothermic, adsorption is spontaneous as it is entropically directed.

4 Methods

Glycidyl methacrylate (GMA) (Aldrich; purity - 97%), divinylbenzene (DVB) (commercial grade, Nitriflex, Brazil), oleic acid PA (B'Herzog, Brazil), sodium hydroxide PA (B'Herzog, Brazil), ferric chloride PA ($FeCl_3$) (Vetec, Brazil), ferrous sulfate PA ($FeSO_4$) (Vetec, Brazil), dichromate potassium PA (Merck); ethanol (commercial grade, Sumatex, Brazil), diphenylcarbazide PA (Merck), benzoyl peroxide PA (Vetec, Brazil), ethylenediamine (Aldrich; purity - 99%) and poly(vinyl alcohol) (AirProducts, hydrolysis degree of 85% and MM = 80,000 to125,000) were used as received.

4.1 Magnetic glycidyl methacrylate-co-divinylbenzene copolymer synthesis

Poly(GMA-*co*-DVB)-M samples were prepared by radical suspension copolymerization. The monomer phase containing the monomer mixture (98 % mol of GMA and 2 % mol of DVB), benzoylperoxide (1 % mol relative to the total monomers), as initiator, and ferric oxide (10 wt%) was suspended in the aqueous phase consisting of 260 g of water and 1.2 g of poly(vinyl alcohol) (PVA). The copolymerization was carried out at 70 °C for 24 h with a stirring rate of 800 rpm.

4.2 Amino magnetic copolymers synthesis

After copolymerization reaction completed, the particles were washed with water and ethanol, kept in ethanol for 12 h and dried at 50 °C for 24 h. The amino functionalization occurred from 2 g of poly(GMA-co-DVB) (R14) reaction with 10 mL of ethylenediamine (EDA), diethylenetetramine (DETA) or triethylenetetramine (TETA) and 25 mL of dimethylformamide at 55 °C, for 72 h, at 300 rpm. The amino copolymers were washed several times with ethanol and water, filtered and dried at 50 °C, for 24 hours.[45]

4.3 Application and evaluation of the adsorption process of magnetic microspheres

The adsorption studies were evaluated using percentage of removal, adsorption capacity, kinetic models, Langmuir and Freundlich adsorption isotherm models and thermodynamic parameters.

4.5. Effect of pH on the Cr (VI) adsorption in the amino magnetic copolymers To evaluate the effect of pH on the Cr(VI) adsorption capacity of magnetic adsorbents, pH values 2, 4, 5, 6, 7, 8, 10 and 12 were tested. Thus, samples of 100 mg of the copolymer were added to 20 mL of 100 mg L^{-1} Cr(VI) solutions at different pH values previously adjusted with NaOH and/or HCl solutions. The system remained under constant stirring at 25 °C in a thermostatic bath for 24 h. After this time, the resin was separated from the medium by the action of a magnet and the supernatant was analyzed by Molecular Absorption Spectrometry (UV-Vis) (λ=540 nm), after reaction of this ion with 1,5-diphenylcarbazide to determine the remaining Cr (VI) content and calculate the removal rate.

4.6. Adsorption kinetics of Cr (VI) in the amino magnetic copolymers

The kinetic models analysis in the adsorption process was carried out in different temperatures 25, 30, 35, 40 and 45 °C. The copolymer mass was 5.0 g.L^{-1} Cr (VI) solution and pH values was established at 2. Samples were shaken and aliquots of the supernatant were removed after different time intervals (0, 5, 10, 30, 60, 90, 120, 150, 180, 210, 240, 270, 300, 360 and 1400 min). The Cr(VI) concentration was determined by Molecular Absorption Spectrometry (UV-Vis) (λ=540 nm), after reaction of this ion with 1,5-diphenylcarbazide. The interpretation of the experimental data and the mechanisms that control the adsorption process was adjusted to the kinetic models, investigated and validated by the correlation coefficients of their linearized equations: [log (qe - qt) vs t] for the pseudo-first order model, [t/qt vs t] for the pseudo-second order model and [qt vs t1/2] for the intraparticle diffusion model.

4.7. Isotherm Adsortion of Cr (VI) in the amino magnetic copolymers

Performance tests were carried out in a constant concentration range (100 mg.L^{-1}) for constant temperatures (298.15K, 303.15K, 308.15K, 313.15K and 318.15K). The adsorption results were fitted to Langmuir and Freundlich models. To calculate the maximum adsorbed capacity (q_{max}) and the adsorption constant (K_L), the Langmuir model was adopted. The experimental points were fitted to the model using the method of least squares (simple linear regression).

Declarations

Acknowledgements. The authors thank Fundação de Amparo à Pesquisa do Estado do Rio de Janeiro (FAPERJ) and Conselho Nacional de Desenvolvimento Científico e Tecnológico (CNPQ) for the financial support.

Contributions. Marcos Antonio da Silva Costa, Prof.: Conceptualization; Data curation; Funding Acquisition; Investigation; Methodology; Supervision; Writing – review & editing. Washington José Fernandes Formiga: Conceptualization; Data curation; Formal analysis; Investigation; Methodology; Visualization; Writing – original draft. Henrique Almeida Cunha: Data curation; Supporting; Formal analysis; Validation; Writing – original draft. Jacira Aparecida Castanharo: Data curation; Investigation; Writing – original draft; Writing – review & editing. Ivana Lourenço de Mello Ferreira: Conceptualization; Data curation; Supervision; Writing – review & editing. Manoel Ribeiro da Silva: Data curation; Supporting; Formal analysis; Validation; Writing – review & editing.

Funding. Marcos Antonio da Sivla Costa, Prof.: Proc. nº E-26-010.000982/2019 (Faperj)
“Cooperative Research Network on Nanostructured Materials and Device Engineering”. Washington José Fernandes Formiga, Manoel Ribeiro da Silva, Henrique Almeida Cunha, Ivana Lourenço de Mello Ferreira and Jacira Aparecida Castanharo – No funding.

Data availability. At the author of correspondence

Conflicts of interest. The authors declare that they have no conflict of interest.

Ethical approval. Not applicable.

References

1. Fungaro, D. A. , Yamaura, M., Graciano, J. E. A.: Remoção de íons Zn^{2+} , Cd^{2+} e Pb^{2+} de soluções aquosas usando compósito magnético de zeólita de cinzas de carvão. Quim Nova, **33**, 1275-1278, (2010).
2. Sharma, A. , D. Mangla, Shehnaz, Chaudhry, S. A.: Recent advances in magnetic composites as adsorbents for wastewater remediation. J. Environ. Manage., **306**, 114483-114500 (2022)
3. Xu, R. , Du, H., Liu, C., Liu, H., Wu, M., Zhang, X., Si, C., Li, B.: An efficient and magnetic adsorbent prepared in a dry process with enzymatic hydrolysis residues for wastewater treatment. J. Clean. Prod., **313**, 127834 (2021)
4. Gunatilake, S. K. : Methods of Removing Heavy Metals from Industrial Wastewater. *J. Multidiscip. Eng. Sci. Studi.*, **1**, 12-18 (2015).
5. Turhanen, P. A. , Vepsäläinen, J. J., Peräniemi, S.: Advanced material and approach for metal ions removal from aqueous solutions. Sci. Rep., **5**, 1-8 (2015)
6. Sthiannopkao, S. , Sreesai, S. : Utilization of pulp and paper industrial wastes to remove heavy metals from metal finishing wastewater. J. Environ. Manage., **90**, 3283-3289 (2009)
7. Aravind, J. , Kanmani, P., Devisri, A. J., Dhivyalakshmi, S. M. : Equilibrium and kinetic study on chromium (VI) removal from simulated waste water using gooseberry seeds as a novel biosorbent. Glob. J. Environ. Sci. Manag., **1**, 233-244 (2015)
8. Dehghani, M. H., Sanaei, D. , Ali, I., Bhatnagar, A.: Removal of chromium(VI) from aqueous solution using treated waste newspaper as a low-cost adsorbent: Kinetic modeling and isotherm studies. J. Mol. Liq., **215**, 671-679 (2016)
9. Rengaraj, S., Yeon, K. H., Moon, S. H.: Removal of chromium from water and wastewater by ion exchange resins. J. Hazard. Mater., , **87**, 273-287 (2001)
10. Qasem, N. A. A., Mohammed, R. H., Lawal, D. U.: Removal of heavy metal ions from wastewater: a comprehensive and critical review. Clean Water, **36**, 1-15 (2021)
11. Ranganathan, K.: Chromium removal by activated carbons prepared from Casurina equisetifolia leaves. Bioresour. Technol., **73**, 99-103 (2000)
12. Furtado, M.: Desmineralização de água.Química e Derivados, **3**, 14-24 (2010)

13. Malović, L., Nastasović, A., Sandić, Z., Marković, J., Đorđević, D., Vuković, Z.: Surface modification of macroporous glycidyl methacrylate based copolymers for selective sorption of heavy metals. J. Mater. Sci., **42**, 3326-3337 (2007)
14. Hercigonja, R. V. , Maksin, D. D., Nastasović, A. B., Trifunović, S. S., Glodić, P. B., Onjia, A. E.: Adsorptive removal of technetium-99 using macroporous poly(GMA-co-EGDMA) modified with diethylene triamine. J. Appl. Polym. Sci., **123**, 1273-11282 (2012)
15. Bruchet, A., Dugas, V., Laszak, I., Mariet, C., Goutelard, F., Randon, J. : Synthesis and Characterization of Ammonium Functionalized Porous Poly(glycidyl methacrylate-co-ethylene dimethacrylate) Monoliths for Microscale Analysis and Its Application to DNA Purification. *J. Biomed.*, **7**, 1-11 (2011)
16. Wieder, W., Bisjak, C. P., Huck, C. W., Bakry, R., Bonn, G. K.: Monolithic poly(glycidyl methacrylate-co-divinylbenzene) capillary columns functionalized to strong anion exchangers for nucleotide and oligonucleotide separation. J. Sep. Sci., **29**, 2478-2484 (2006)
17. Nastasovic, A., Sandic, Z. P., Surucic, L., Maksin, D., Jakovljevic, D., Onjia, A.: Kinetics of hexavalent chromium sorption on amino-functionalized macroporous glycidyl methacrylate copolymer. J. Hazard. Mater., **171**, 153-159 (2009)
18. Donia, A. M., Atia, A. A., Moussa, E. M., El-Sherif, A. M., El-Magied, M. O.: Removal of uranium(VI) from aqueous solutions using glycidyl methacrylate chelating resins. Hydrometallurgy, **95**, 183-189 (2009)
19. Jin, J. M., Lee, J. M., Há, M. H., Lee, K., Choe, S.: Highly crosslinked poly(glycidyl methacrylate-co-divinyl benzene) particles by precipitation polymerization Polymer, **48**, 3107-3115 (2007)
20. Wang, K., Qiu, G., Cao, H., Jin, R.: Removal of Chromium (VI) from Aqueous Solutions Using Fe3O4 Magnetic Polymer Microspheres Functionalized with Amino Groups. Materials, **8**, 8378-8391 (2015)
21. Zhao, Y. G., YU, S. H., Dong, P. S.,. Qin, H. M.: Synthesis, characterization and properties of ethylenediamine-functionalized Fe_3O_4 magnetic polymers for removal of Cr(VI) in wastewater. J. Hazard. Mater., **182**, 295-302 (2010)
22. Formiga, W. J. F., Costa, M. A. S., Silva, M. R., Souza, J. V. S., Ferreira, I. L. M.: Preparation of Magnetic Poly(glycidyl Methacrylate-*Co*-Divinylbenzene) Microspheres with amino or Quaternary Groups for Cr(VI) Removal from Aqueous Solutions Int. J. Sci. Res., **2**, 126-133 (2016)
23. Santa Maria, L. C., M. Leite, M. C. A., Costa, M. A. S., Ribeiro, J. M. S., Senna, L. F., Silva, M. R., Characterization of magnetic microspheres based on network styrene and divinylbenzene copolymers. Mater. Lett., **58**, 3001-3006 (2004)
24. Castanharo, J. A., Ferreira, I. L. M., Costa, M. A. S., Silva, M. R., Costa, G. M., Oliveira, M. G.: Magnetic microspheres based on poly(divinylbenzene-co-methyl methacrylate) obtained by suspension polymerization. Polímeros, **25**, 192-199 (2015)
25. Formiga, W. J. F., Silva, M. R., Cunha, H. A., Castanharo, J. A., Ferreira, I. L. M., Costa, M. A. S.: Influence of Benzoyl Peroxide and Divinylbenzene Concentrations on the Properties of Poly(glycidyl methacrylate-*co*-divinylbenzene) Magnetic Microspheres. Macromol. React. Eng., **17**, 1-6 (2023)
26. Chung, T., Pan, H., Lee, W. : Preparation and application of magnetic poly (styrene-glycidyl methacrylate) microspheres.J. Magn. Magn., **311**, 36-40 (2007)
27. Lee, Y., Rho, J., Jung, B.: Preparation of magnetic ion-exchange resins by the suspension polymerization of styrene with magnetite. J. Appl. Polym. Sci., **89**, 2058-2067 (2003)
28. Santa Maria, L. C., Costa, M. A. S., Soares, J. G. M., Wang, S. H., Silva, M. R.: Preparation and characterization of manganese, nickel and cobalt ferrites submicron particles in sulfonated crosslinked networks. Polymer, **46**, 11288-11293 (2005)
29. Shoaib, A., Bajwa, R., Shafique, U., Removal of heavy metals by adsorption on Pleurotus ostreatus. J. Anwar. Biomass Bioenergy, **35**, 1675-1682 (2011)
30. Bayramoglu, G., Celik, G., Yılmaz, M., Arica, M. Y.: Modification of surface properties of Lentinus sajor-caju mycelia by physical and chemical meth- ods: evaluation of their Cr^{6+} removal efficiencies from aqueous medium. J. Hazard. Mater., **119**, 219-229 (2005)
31. Bayramoglu, G., Arica, M. Y.: Adsorption of Cr(VI) onto PEI immobilized acrylate-based magnetic beads: Isotherms, kinetics and thermodynamics study J. Chem. Eng., **139**, 20-28 (2008)
32. Gurgel, L. V. A., Melo, J. C. P., Lena, J. C., Gil, L. F.: Adsorption of chromium (VI) ion from aqueous solution by succinylated mercerized cellulose functionalized with quaternary ammonium groups. Bioresour. Technol., **100**, 3214-3220 (2009)

33. R. J. Hunter, Introduction to modern colloid science. New York: Oxford University Press, 1993.
34. Atia, A. A., Donia, A. M., El-Enein, S. A., Yousif, A. M.: Effect of chain length of aliphatic amines immobilized on a magnetic glycidyl methacrylate resin towards the uptake behavior of Hg(II) from aqueous solutions. Sep. Sci. Technol., **42(2)**, 403-420 (2007)
35. Atia, A. A., Donia, A. M., Yousif, A. M.: Removal of some hazardous heavy metals from aqueous solution using magnetic chelating resin with iminodiacetate functionality.Sep. Purif. Technol., **61**, 348-357 (2008)
36. Huang, S. H., Chen, D. H.: Rapid removal of heavy metal cations and anions from aqueous solutions by an amino-functionalized magnetic nano-adsorbent. J. Hazard. Mater., **163**, 174-179 (2009)
37. Maksin, D. D., Nastasović, A. B., Nikolić, A. D. M., Surućić, L. T., Sandić, Z. P., Hercigonja, R. V., Onjia, A. E.: Equilibrium and kinetics study on hexavalent chromium adsorption onto diethylene triamine grafted glycidyl methacrylate based copolymers. J. Hazard. Mater., **209–210**, 99-110 (2012)
38. Sun, G., Xu, X.: Sunflower stalks as adsorbents for color removal from textile wastewater. *Ind. Eng. Chem. Res.*, **36**, 808-812 (1997)
39. Marjanović, V., Lazarević, S., Janković-Častvan, I., Potkonjak, B., Janaćković, D.: Adsorption of chromium(VI) from aqueous solutions onto amine-functionalized natural and acid-activated sepiolites. Appl. Clay Sci., **80–81**, 202-210 (2013)
40. Toledo, T. V., Bellato, C. R., Pessoa, K. D., Fontes, M. P. F.: Remoção De Cromo (Vi) De Soluções Aquosas Utilizando O Compósito Magnético Calcinado Hidrotalcita- Óxido De Ferro: Estudo Cinético E De Equilíbrio Termodinâmico. Quim Nova, 36, 419-425 (2013)
41. Ho, Y. S., Mckay, G.: The kinetics of sorption of divalent metal ions onto Sphagnum moss peat.Water Res., **34**, 735-742 (2000)
42. Ghasemlou, S., Aghaire, H., Monajjemi, M.: Thermodynamic Study of Hg (II) Ion Adsorption onto Nano Hydroxyapatite from Aqueous Solution. J. Phys. Theor. Chem., **10**, 125-136 (2013)
43. Hu, X., Wang, J. S., Liu, Y. G., Li, X., Zeng, G. M., Bao, Z., Zeng, X., Chen, A., Long, F.: Adsorption of chromium (VI) by ethylenediamine-modified cross-linked magnetic chitosan resin: Isotherms, kinetics and thermodynamics. J. Hazard. Mater., **185**, 306-314 (2011)
44. Venugopal, V., Mohanty, K.: Biosorptive uptake of Cr(VI) from aqueous solutions by Parthenium hysterophorus weed: Equilibrium, kinetics and thermodynamic studies. J.Chem. Eng., **174**, 151-158 (2011)
45. Paredes, B., González, S., Rendueles, M., Villa-Garcia, M. A., Díaz, J. M.: Egg-white protein fractionation using new weak anion-exchange resins based on Poly(Glycidyl Methacrylate-co-Ethylendimethacrylate). Preparation and characterization. *J Chromatogr Sci.*, **43**, 241-248 (2005)

Figures

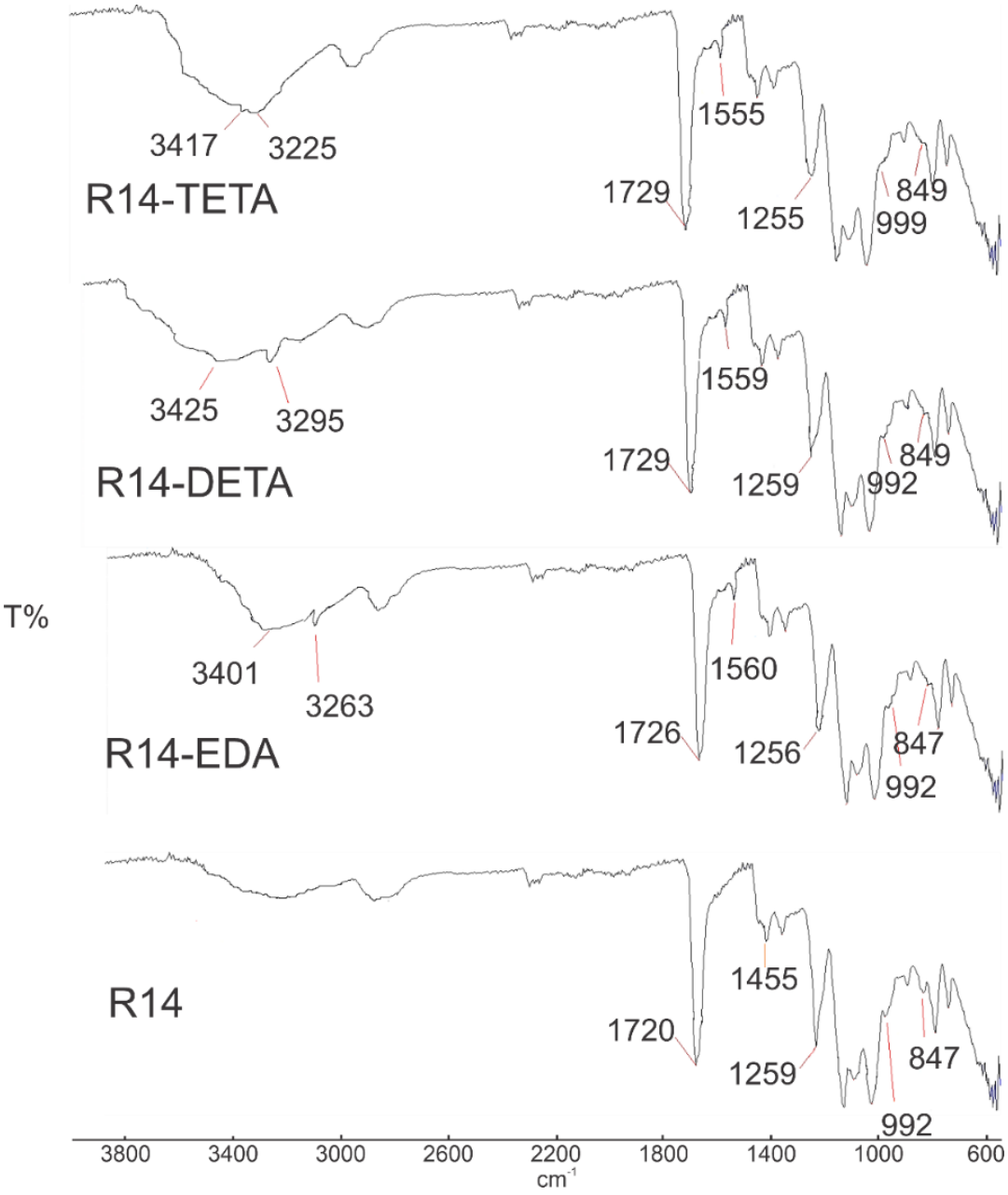

Figure 1

P(GMA-*co*-DVB)-M FTIR-ATR spetra before (R14) and after functionalization with ethylenediamine (R14-EDA), diethylenetriamine (R14-DETA) and triethylenetetramine (R14-TETA)- R14: GMA/DVB = 98/2; BPO = 1%; iron oxide = 10%; T = 80 °C).

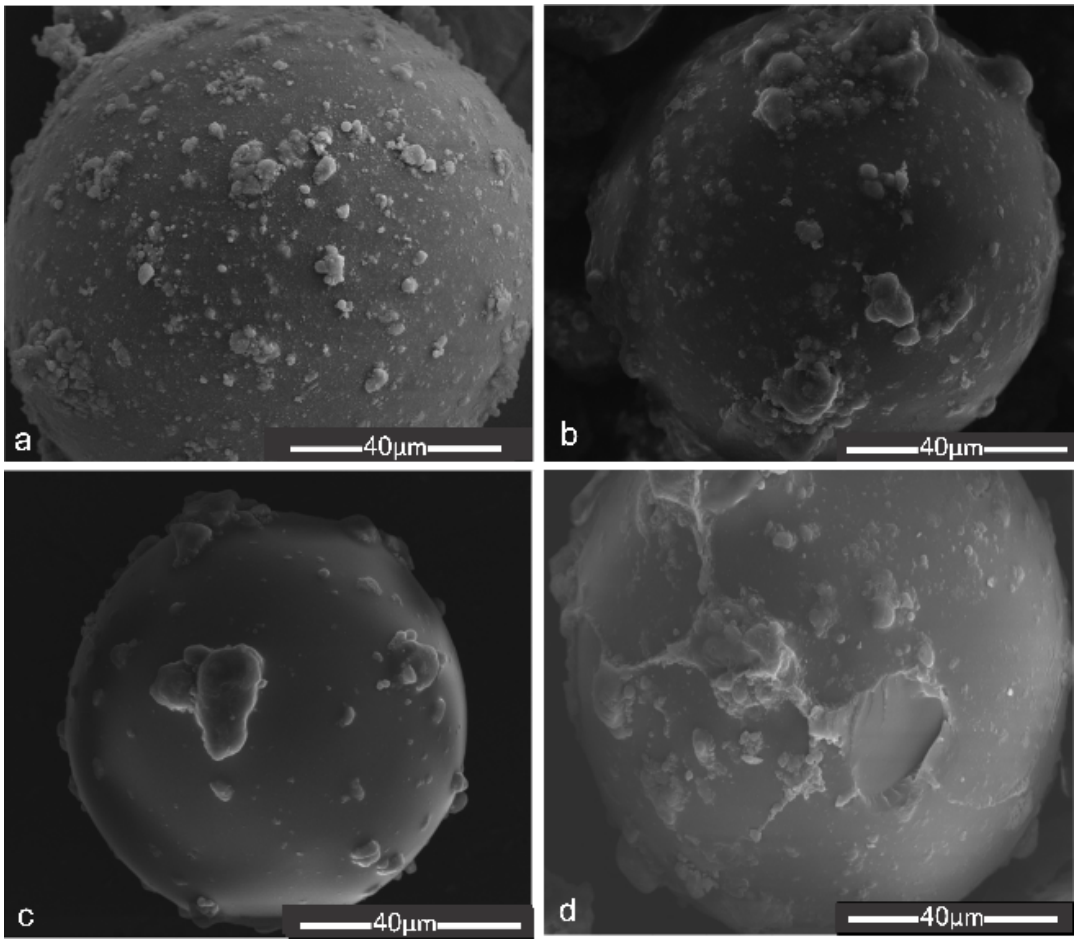

Figure 2

P(GMA-*co*-DVB)-M SEM images: a) before (R14) and functionalization with b) ethylenediamine (R14-EDA), c) diethylenetriamine (R14-DETA), and d) triethylenetetramine (R14-TETA) (2500x magnification, R14: GMA/DVB = 98/2; BPO = 1%; iron oxide = 10%; T = 80 °C).

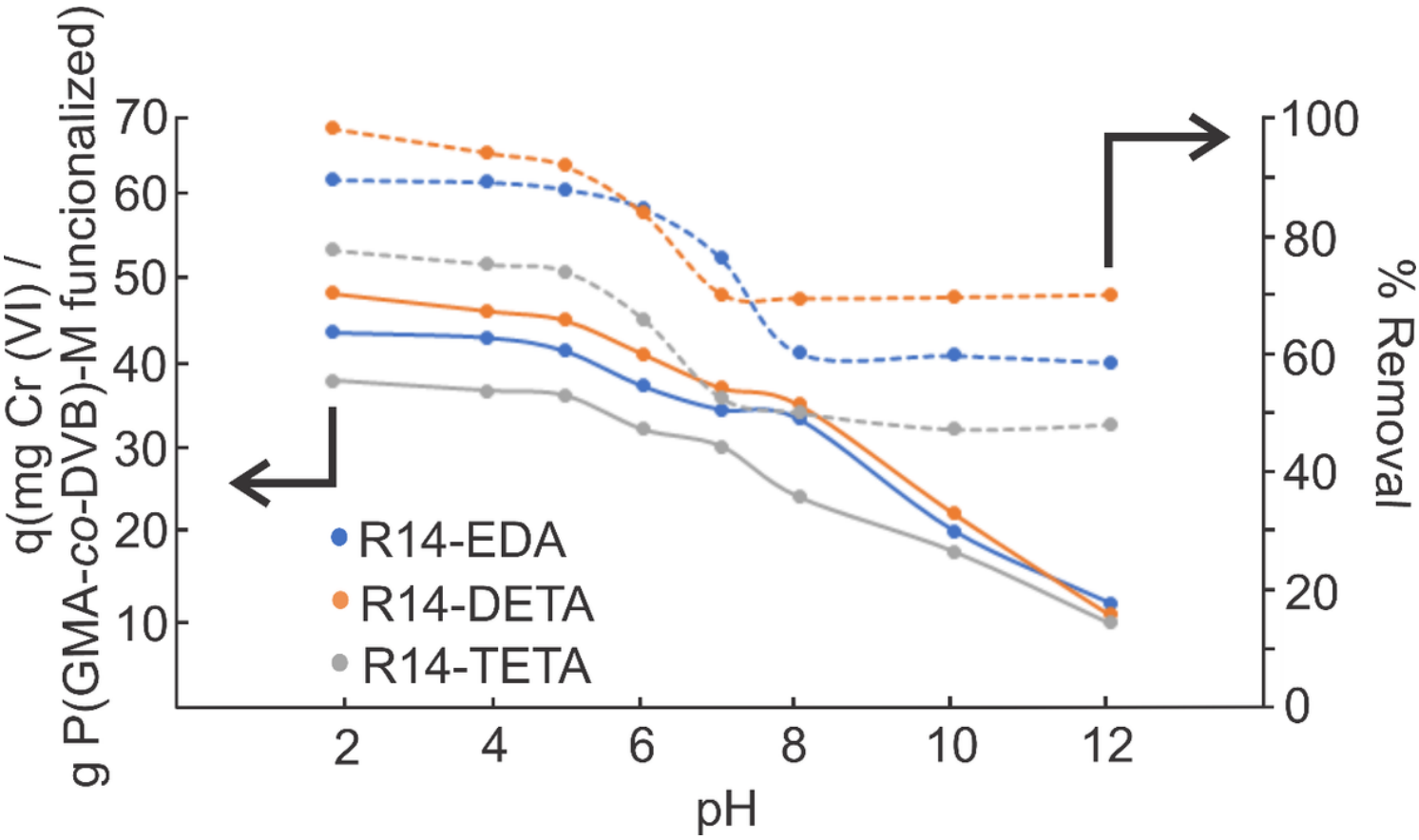

Figure 3

Effect of pH on the Cr (VI) adsorption by P(GMA-*co*-DVB)-M: functionalization with ethylenediamine (R14-EDA), diethylenetriamine (R14-DETA) and triethylenetetramine (R14-TETA) (C_0 = 100 mg.L^{-1} ; Volume = 50 mL; R14-EDA = R14-DETA = R14-TETA = 5 g.L^{-1}; stirring speed = 200 rpm; temperature = 25 °C., 24h).

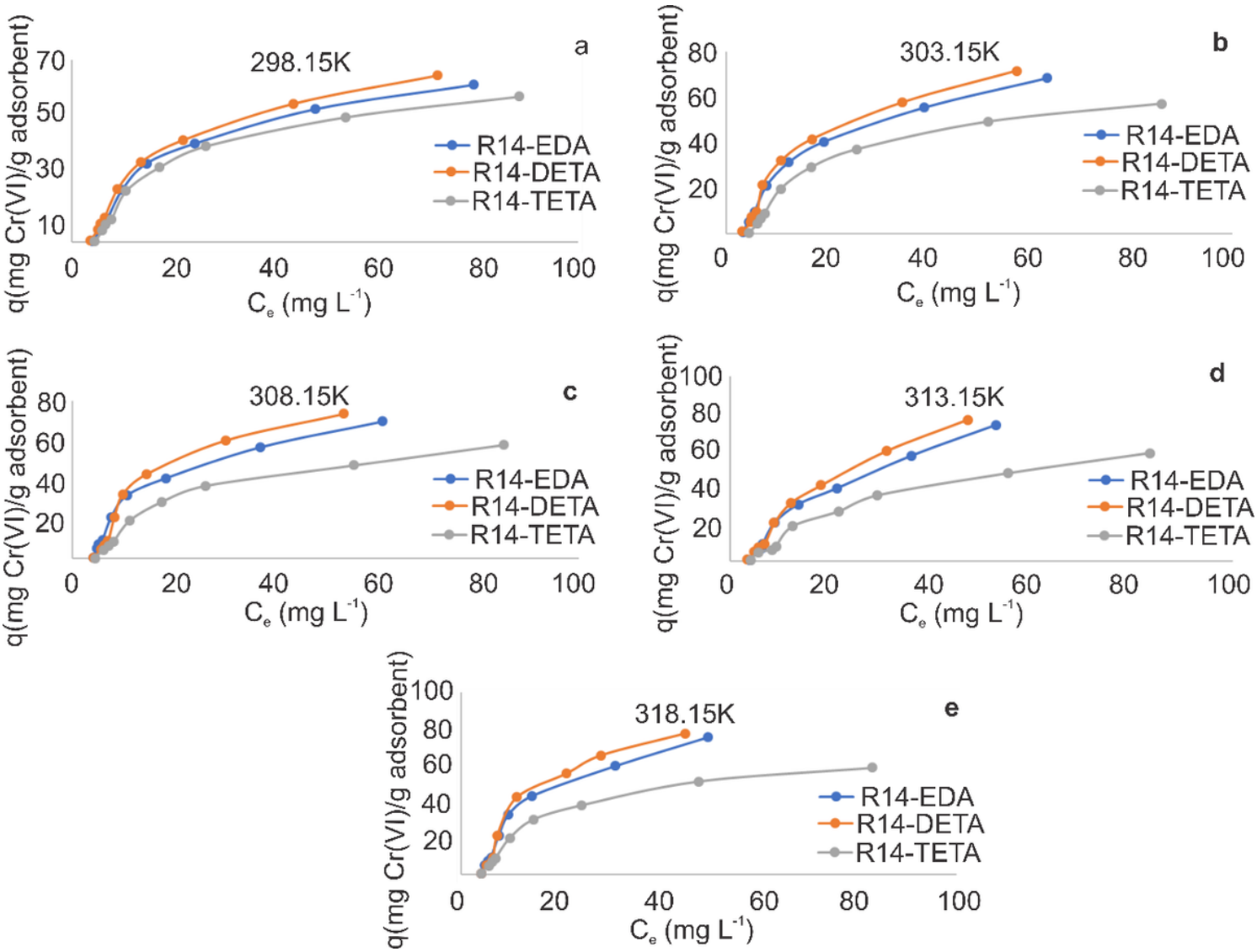

Figure 4

Adsorption isotherms of Cr (VI) adsorption by P(GMA-co-DVB)-M: functionalization with ethylenediamine (R14-EDA), diethylenetriamine (R14-DETA) and triethylenetetramine (R14-TETA) at different temperatures, 24h, pH=2

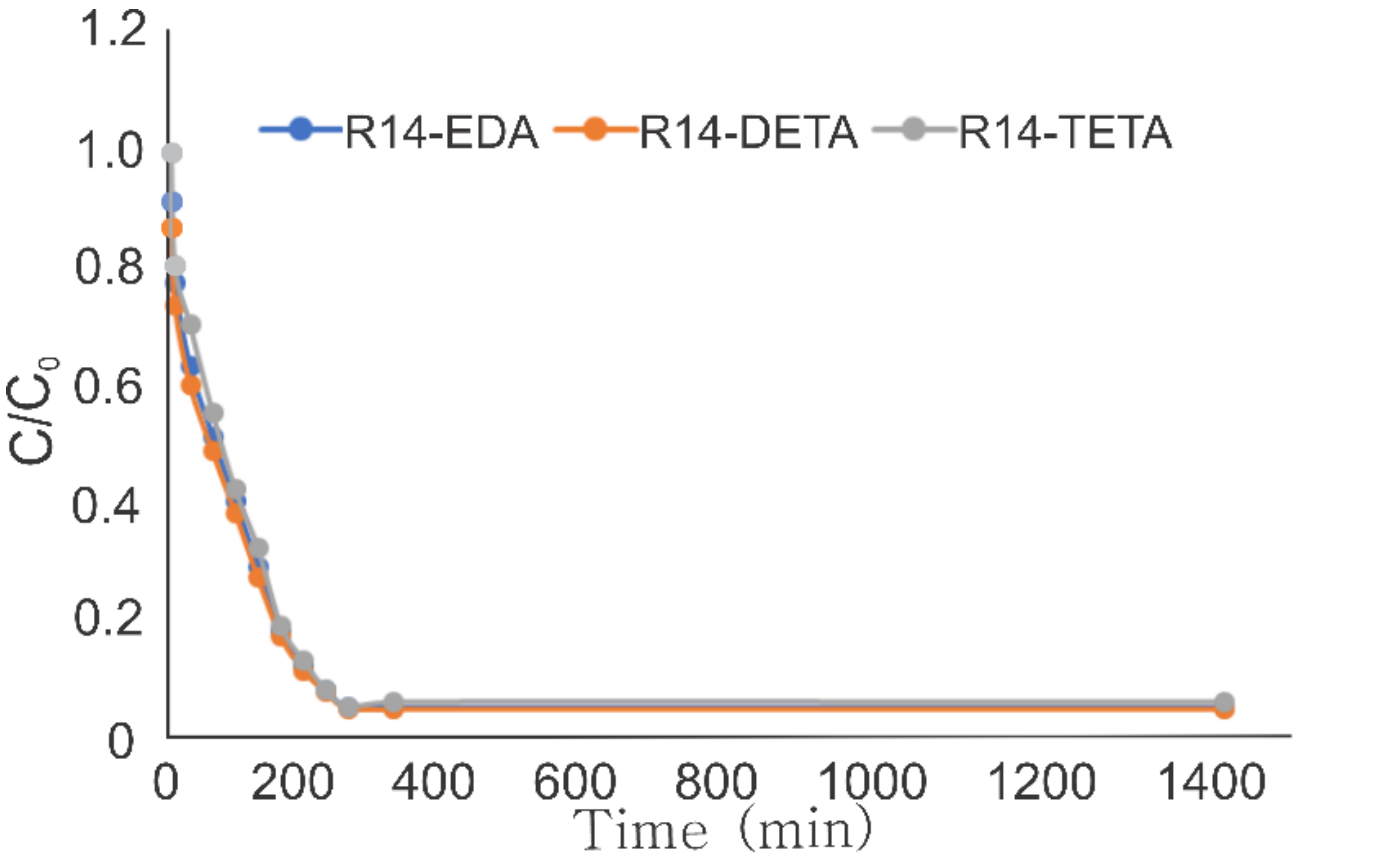

Figure 5

Effect of contact time on Cr (VI) adsorption by P(GMA-*co*-DVB)-M (5,0g.L^{-1}) functionalization with ethylenediamine (R14-EDA), diethylenetriamine (R14-DETA) and triethylenetetramine (R14-TETA). (C_o – initial concentration of Cr (VI); C - concentration at any given time; at 25°C; pH=2; 200rpm; C_0=100mg/L)